Chapter 6

Specific Emitter Identification Based on Fractal Features

Janusz Dudczyk

Additional information is available at the end of the chapter

http://dx.doi.org/10.5772/67894

Abstract

If we take into consideration the fact that the radar signal recognition and identification process is an integral part of contemporary combat operations, the importance of the fractal analysis increases significantly. For this reason, the fractal analysis is used in the process of radar sources identification on the contemporary battlefield. Radar Signal Recognition (RSR) with the use of classical methods, that is based on statistical analysis of basic measurable parameters of a radar signal, such as Radio Frequency (RF), Amplitude (A), Pulse Width (PW) or Pulse Repetition Interval (PRI) is not enough to carry out the distinction process of particular copies of the same radar type. Only by this approach, the identification process of particular copies in a set of the same type emitters can be carried out. As a result, it is possible to maximize Correct Identification Coefficient (CIC) in the final stage of the recognition process, which is realized in Electronic Warfare (EW) systems. One of the most important elements of the whole recognition and identification process, which is realized in ELectronic INTelligence (ELINT) battlefield system, is building a measurement data vector, then a radar's metrics and the same database. This approach is called Specific Emitter Identification (SEI).

Keywords: fractal feature, pattern of radar, Specific Emitter Identification (SEI), radar vector parameters, ELINT system, Radar Signal Recognition (RSR), Correct Identification Coefficient (CIC)

1. Introduction

Developing an innovative method for generating distinctive features extracted from radar signals in order to achieve explicit identification is a main goal in the process of Specific Emitter Identification (SEI). As a result, it is possible to maximize Correct Identification Coefficient (CIC) and identify particular copies of radars of the same type in ELectronic INTelligence (ELINT) system on the contemporary battlefield. The presented achievements in this

chapter concern methods and techniques adjusted to electromagnetic emitter source recognition and identification with particular reference to the systematic approach, that is, from the acquisition process, through initial data transformation, main transformation, classification and identification and building a model in the DataBase (DB). Only a comprehensive approach can be coherently fitted into a harmonious whole of all the ELINT recognition systems' processes on the contemporary battlefield. As a result, this approach may contribute to an increase in effectiveness of activity by minimization of time, which is necessary for the decision process realized in Electronic Warfare systems.

Generally, it is possible to distinguish the main task, which has a significant contribution to the development of recognition and identification of radar signals, that is, developing innovative methods for generating distinctive features of radar signals [1–5]. As mentioned above, the task is connected with developing a method for setting the structure of basic measurable parameters of a radar signal in the form of time-frequency-formalized Pulse Descriptive Word (PDW) [5, 6], developing and implementing in SEI process, an advanced Hierarchical Agglomerative Clustering Algorithm (HACA) based on the 'bottom up' agglomerative formula, which makes it possible to receive dendrograms of hierarchical clustering for pulse repetition intervals and their distinctive analysis [1], applying the inter-pulse modulation analysis to extract distinctive features [7], developing an innovative histogram procedure to build PRI decomposition [2] and finally developing an innovative method for defining a transformation attractor of radar signals measurement clusters [3, 4]. This approach is called Specific Emitter Identification.

2. Classic recognition of radar signals

As a general rule, the systems aiming at acquisition, analysis and recognition of radar signals on the contemporary battlefield are autonomous systems, which are made of electronic recognition devices doing ELINT tasks. These systems accomplish complex procedures in the scope of emission acquisition, analysis, transformation and radar emission recognition with the range of wavelengths 0.5–18 GHz, long-term data archivization and full synthesis and fusion of information. These systems, in most cases, are made of the following subsystems and modules, that is, radar signal acquisition subsystem, radar signal processing and analysis subsystem, database management subsystem and communication module[1] between particular subsystems.

Accomplishing basic tasks in the designed systems of radar signal acquisition, analysis and recognition on the contemporary battlefield is based on:

- automated searching for and detecting[2] electromagnetic emitters (in the range of wavelengths 0.5–18 GHz);

[1]Communication module between particular subsystems and components of acquisition system and radar signal analysis on the contemporary battlefield is not the subject of this chapter.

[2]In the aspect of tasks connected with searching for and detecting signals and measuring their parameters, the specialist equipment of the radar signal acquisition, analysis and recognition system makes it possible to accomplish the tasks above on the land, from the air or the sea and may be adjusted to a plane, helicopter, a ship or installed in a special container case.

http://dx.doi.org/10.5772/67894

- automated parameter measurement of the detected emitters;
- analysis of measured signal parameters in a thick electromagnetic environment (a few thousand or more pulses) and initial measurement data processing (initial parametric selection and/or signal reduction);
- main signal processing (extraction of basic features and estimation of basic measurable radar signal parameters i.e. signal radio frequency, amplitude, pulse width, pulse repetition interval) on the basis of statistical functions concerning estimating e.g. average values of parameters, class models and hypothesis verification;
- radar signal archivization in files with measurement data in the DataBase and updating procedure as well as DataBase structure modification;
- radar types recognition and classification on the basis of radar signals received from them by comparing signal parameters with the model in BD in the shortest time possible and using expert's knowledge in the process of emitter sources recognition, classification and location;
- visualization of signals, measurement data clusters, results of recognition and other data and distinctive information presented in a tabular and graphic form;
- depict results of recognition on a digital map and automatically adjusting a unit to the area;
- possibilities of import and analysis of measurement data from electronic recognition, which is received from other sources and data measurement and recognition information fusion;
- creating a simulation software to generate warfare scenarios, test correctness of emission sources classification, recognition and location procedures and to estimate the effectiveness of the system and trainings for operators.

The analysis of radioelectronic situation on the contemporary battlefield and long-term radar signal measurements makes it possible to admit that during the process of signal recognition and classification, there is a phenomenon of penetrating ranges of radar parameters, many ranges of particular parameters for single radars, different types of emissions (constant, pulse, interrupting), complexity of sounding pulses and specific work properties (signal polarization depending on the weather), decrease in frequency of repetition and top pulse as the beams go above the horizon or the change of top power in case of e.g. weather condition changes. The general block diagram of radar signal acquisition, analysis and recognition is presented in **Figure 1**.

The radar recognition system (see **Figure 1**) is only able to recognize and classify particular types of radars. A definitely more advanced one is the recognition process understood in a 'narrow sense'. Its aim is to identify these signals, thus their emission sources as well. I deal with the recognition understood in a 'narrow sense', which concerns identification of particular radar copies of the same type depending on the detail level.

The process of distinguishing the radar emission source even 'a single copy' is the exact identification of radar signal source in the aspect of SEI. Thus, applying in the acquisition system, the

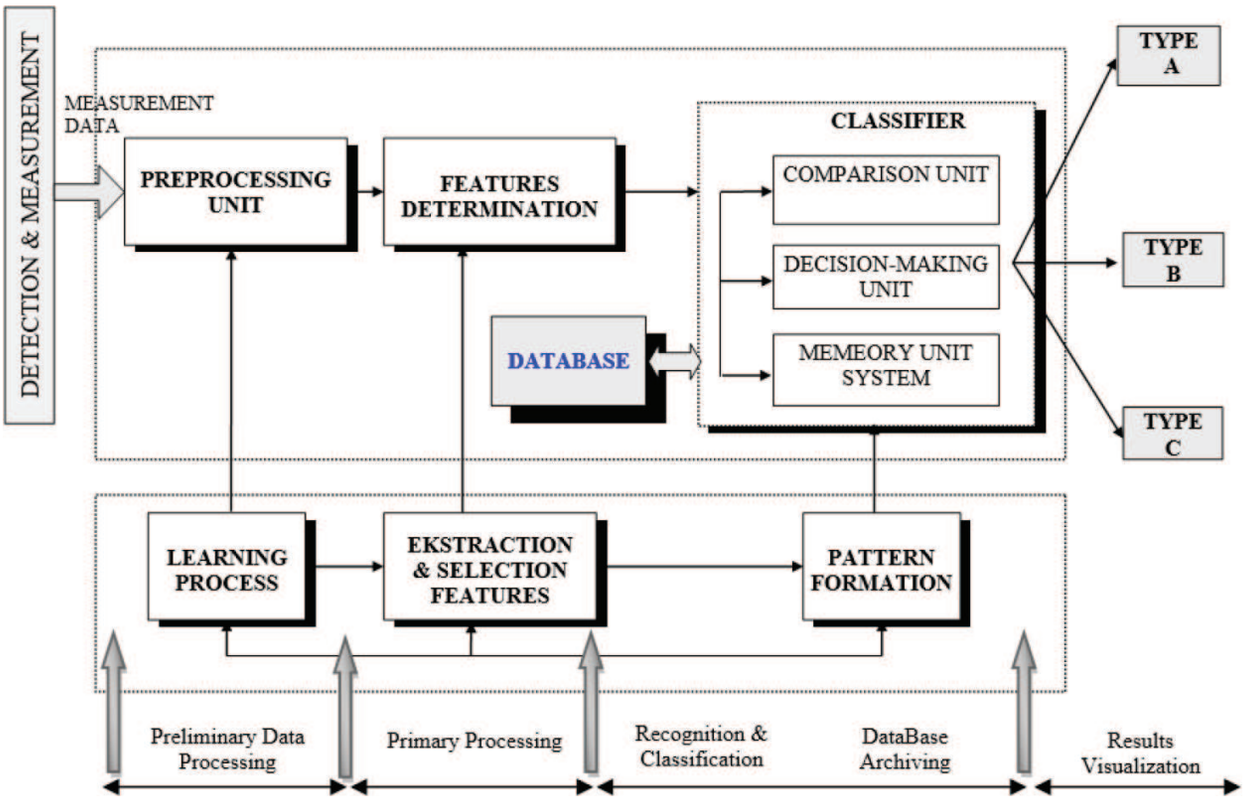

Figure 1. The process of information processing in the radar recognition system.

analysis and recognition of radar signals, inter-pulse analysis of signal parameters (defining the type of inter-pulse modulation and estimation of parameters' modulation), intra-pulse analysis (defining the type and parameters of intra-pulse modulation on the basis of a single pulse), applying innovative methods for generating distinctive features, using fast-decision identification algorithm and advanced DataBases prepared as a result of modelling entity relationships and using AI[3] devices is an immanent specificity of ELINT systems and makes it possible to identify particular copies of radar emitters with the use of the above dedicated methods for generating distinctive features' signals in Electronic Warfare (EW) systems. As concerns contemporary used ELINT class systems, data classification and recognition techniques are currently developed fields of science, it is not possible to formulate optimal model of their structure and maximize the recognition and classification function as well as the identification function.

In **Figure 2**, a block diagram of the acquisition, analysis and identification system, including the subsystems that implement modern and advanced methods for generating distinctive fractal features, is presented.

[3]AI (Artificial Intelligence), a term of artificial intelligence, which in BD systems is realized on the basis of using artificial neural networks (so-called AI bionic trend) and expert systems, based on predicate calculus (so-called AI pragmatic trend).

http://dx.doi.org/10.5772/67894

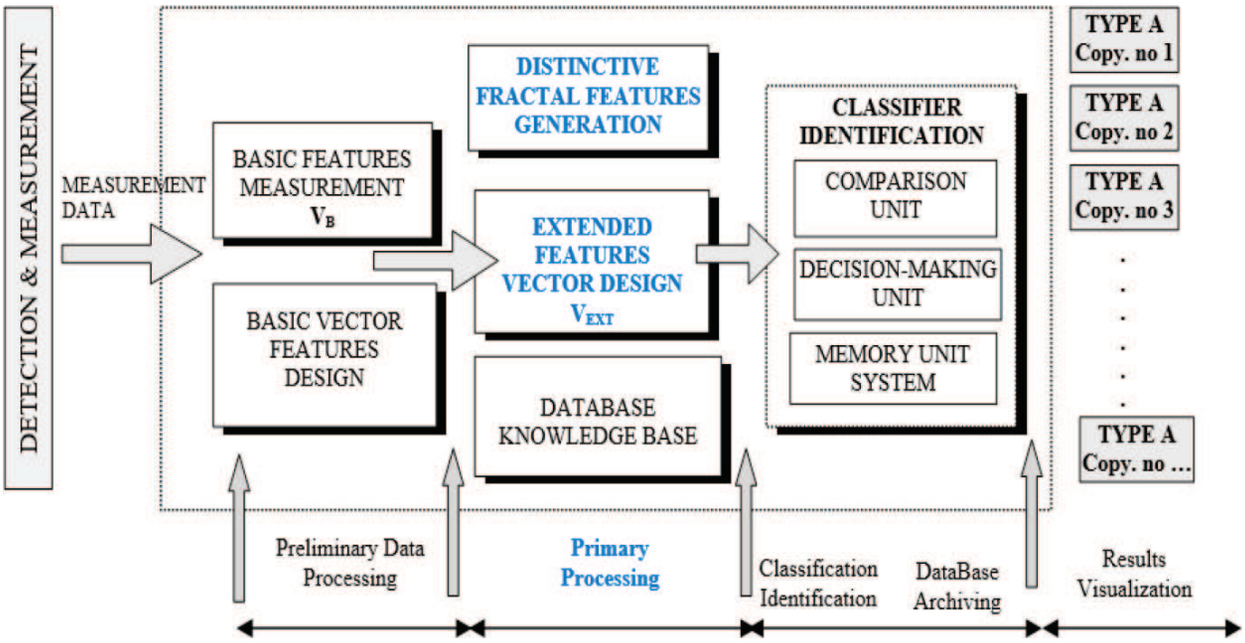

Figure 2. The process of distinctive fractal features generation in the RSR system.

3. Innovative method for generating distinctive features based on fractal analysis

RSR with the use of classic techniques, which are based on the statistical analysis of basic measurable parameters, such as radio frequency, signal amplitude, pulse width, and pulse repetition interval, is completely not sufficient for SEI process to carry out the process of distinguishing particular radar copies of the same type.

For this reason, on the stage of initial data processing, a method for defining the structure of basic measurable parameters of a radar signal in the form of formalized time-frequency Pulse Description Word was developed. These vectors are input data into the further process of generating distinctive features, in the main processing stage [3, 4]. As mentioned above, the PDW vector is a formalized data structure of record type, where particular fields consist of frequency parameters and time parameters of radar signal according to Eq. (1), where Nr(k) is the number kth of the pulse, $t_p(k)$ is the time of appearing kth pulse in [μs], A(k) is the amplitude of kth pulse, PW(k) is the width of kth pulse in [μs], PRI(k) is the Pulse Repetition Interval of kth pulse in [μs], RF(k) is the Radio Frequency of kth pulse in [MHz], n is the number of pulses in the record of these which are qualified to the analysis while k is the number of pulses in the measured sample.

$$\mathbf{PDW} = \begin{bmatrix} \mathrm{Nr}(1) & t_p(1) & A(1) & \mathrm{PW}(1) & \mathrm{PRI}(1) & \mathrm{RF}(1) \\ \mathrm{Nr}(2) & t_p(2) & A(2) & \mathrm{PW}(2) & \mathrm{PRI}(2) & \mathrm{RF}(2) \\ \cdots & \cdots & \cdots & \cdots & \cdots & \cdots \\ \mathrm{Nr}(k) & t_p(k) & A(k) & \mathrm{PW}(k) & \mathrm{PRI}(k) & \mathrm{RF}(k) \\ \cdots & \cdots & \cdots & \cdots & \cdots & \cdots \\ \mathrm{Nr}(n) & t_p(n) & A(2) & \mathrm{PW}(n) & \mathrm{PRI}(n) & \mathrm{RF}(n) \end{bmatrix} \quad (1)$$

The effect of the further transformation of PDW vector is Basic Signal Vector $\mathbf{V_B}$, whose fields are of particular signal frequency and time parameters, according to Eqs. (2)–(4). The time parameters of the vector $\mathbf{V_B^{PRI}}$ are as follows: minimum pulse repetition interval value $PRI_{\min}$, average pulse repetition interval value PRI_{EV}, maximum pulse repetition interval value $PRI_{\max}$, the number of values of pulse repetition interval $nPRI$, the number of values of average pulse repetition interval $nPRI_{EV}$, the minimum value of pulse width $PW_{\min}$, the average value of pulse width PW_{EV} and the maximum value of pulse width $PW_{\max}$.

$$\mathbf{V_B^{PRI}} = [PRI_{\min}, PRI_{EV}, PRI_{\max}, nPRI, nPRI_{EV}, PW_{\min}, PW_{EV}, PW_{\max}] \tag{2}$$

The frequency parameters of the signal vector $\mathbf{V_B^{RF}}$ are defined according to Eq. (3) and are as follows: the minimum value of the signal radio frequency $RF_{\min}$, the average value of the radio frequency for the period RF_{EV}, the maximum value of the radio frequency in the period of changes $RF_{\max}$, the number of values of the radio frequency nRF and the number of average radio frequencies in the cycle of changes nRF_{EV}.

$$\mathbf{V_B^{RF}} = [RF_{\min}, RF_{EV}, RF_{\max}, nRF, nRF_{EV}] \tag{3}$$

The vector $\mathbf{V_B}$ of the final structure presented according to Eq. (4) consists of parameters concerning information about the accuracy measurements of: radio frequency *sigRF*, pulse repetition interval *sigPRI* and pulse width *sigPW*.

$$\mathbf{V_B} = [\mathbf{V_B^{PRI}}, \mathbf{V_B^{RF}}, sigRF, sigPRI, sigPW] \tag{4}$$

These parameters are the base for defining the brackets of acceptable changes of radar signal, that is, *RF, PRI* and *PW* are used in the estimation process of effectiveness of the Fast decision Identification Algorithm (FdIA), described in [6]. The process of developing the signal vector $\mathbf{V_B}$ also undergoes the process of implementation and automation in the stage of initial data

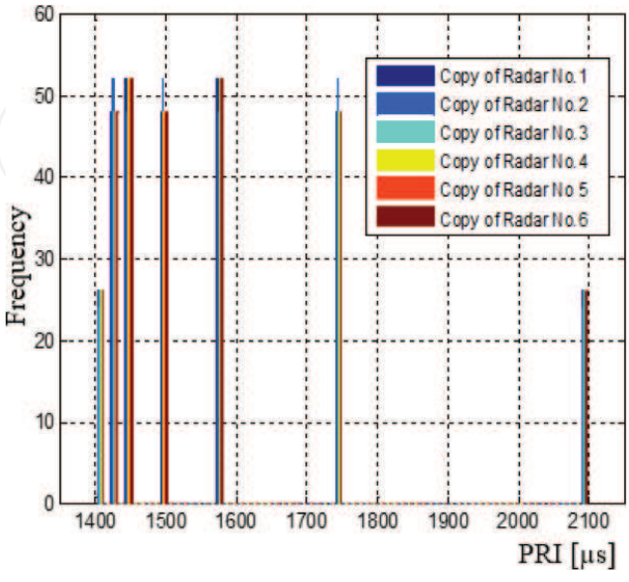

Figure 3. PRI histogram for six copies of the same type of radars marked by colours.

http://dx.doi.org/10.5772/67894

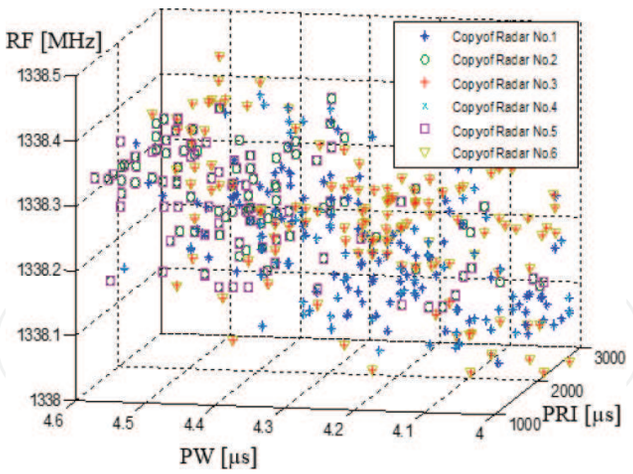

Figure 4. 3D graphic depicting of PW, PRI and RF for six copies of the same type of radars.

processing and the main data processing by ELINT system (see **Figure 2**). During the analysis, in total hundreds of radar samples coming are carried out. The received record collections (e.g. six copies of the same type of radars) with basic measurable parameters of PDW are presented in the form of a graph with basic measurable parameters, that is, RF, PW and PRI in **Figures 3** and **4**. **Figure 3** presents the PRI histogram of six tested radar copies in an overall depiction. **Figure 4** presents a 3D graph of RF, PRI and PW parameters from six copies, in an overall depiction as well.

Figures 5 and **6** present 3D depicting of radio frequency and pulse width for three selected copies of the same type of radars received with the use of 'mesh' function in the MatLab software.

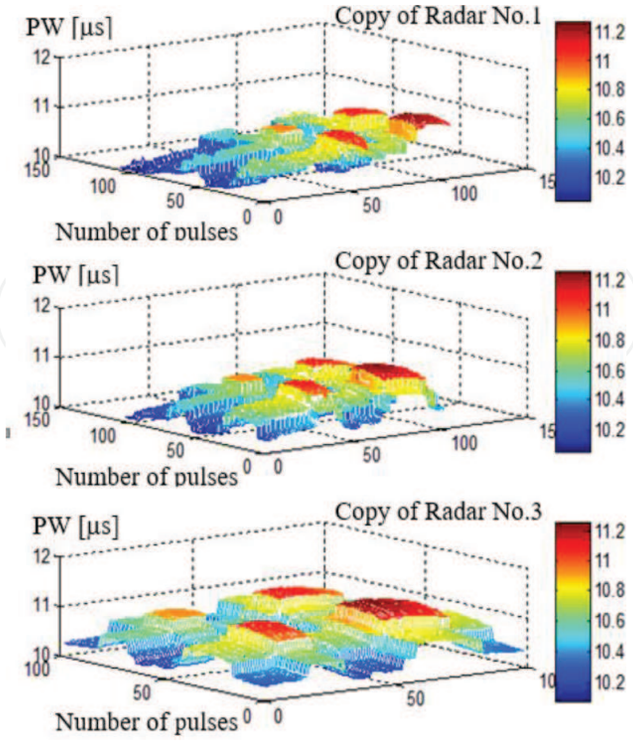

Figure 5. 3D graphic depicting of PW for three selected copies of the same type of radars.

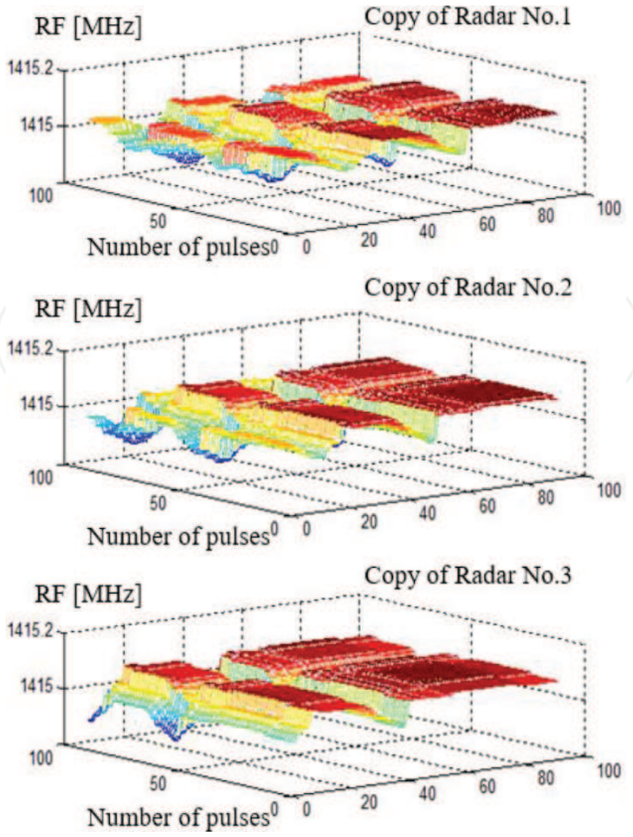

Figure 6. 3D graphic depicting of RF for three selected copies of the same type of radars.

On the basis of the recordings and initial analysis to further process of identification, only these copies were admitted whose basic measurable parameters, that is, RF, PW and PRI were much the same—see **Figures 5–8**. **Figures 5–8** present the biggest similarity of the radar signal parameters which those sources generated.

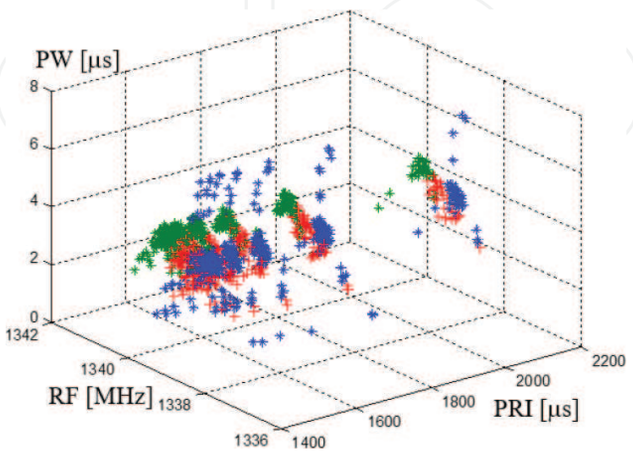

Figure 7. 3D graphic depicting of RF, PRI and PW for three selected copies of the same type of radars marked by three shades of gray.

http://dx.doi.org/10.5772/67894

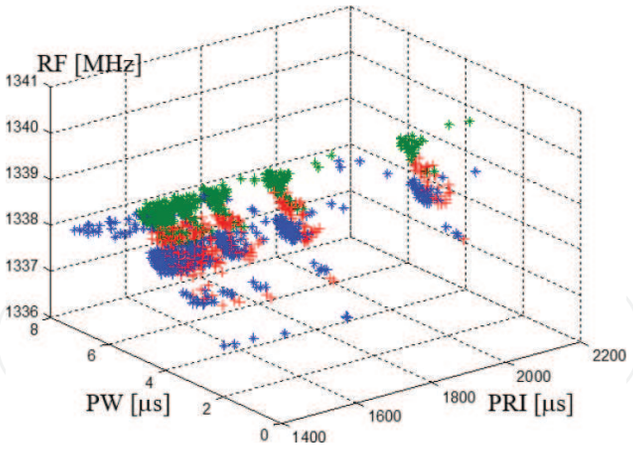

Figure 8. 3D graphic depicting of PW, PRI and RF for three selected copies of the same type of radars marked by three shades of gray.

4. Defining the transformation attractor and distinctive features extraction

One of the ways to increase the number of details of definition is specific identification of electromagnetic emitter sources SEI which extracts distinctive features in the process of signal transformation. The distinctive features may be a result of the received transformations of measurement data sets. New data sets will have fractal features which will make it possible to define clearly the source of radar emission. The fractal features and the theory of fractals is adopted by researchers, especially in the field of SAR (*Synthetic Aperture Radar)* image transformation [8, 9], acoustic signal transformation and the analysis of radar signals. New possibilities of Digital Signal Processing (DSP) in Frequency Modulated Continuous Wave (FMCW) radar and fractal image compression is a promising brand new compression method [10, 11]. It should be noted that the identification of emitter sources based on classical methods of the analysis of basic parameters is currently inefficient. The methods of SEI [12, 13] should be used in order to identify, more precisely, a radar copy of the same type.

4.1. An attractor of transformation

The easiest way to make fractals is by using a set of affine transformations, which are contractions or narrowing transformations. In this case, the set of affine transformations is Iterated Function System (IFS). A recording of radar signal was made. Further frequency values, for which the recording was made, correspond to particular measurement points. By transforming the sets of measurement points in the scope of their symmetry or left-side/right-side asymmetry, what was received was the attractor of transformation which can be a fractal in a special case. As a result, the attractor of generalized measurement function appeared, which was the result of the procedure of SEI described here. While doing the analytical procedure of defining the attractor of measurement function, right-side measurement vectors $\mathbf{p}^{\mathrm{r}}$ and left-side ones $\mathbf{p}^{\mathrm{l}}$ with the beginning in the particular point of reference f_0, so that $\mathbf{p}^{\mathrm{r}} = [p_1^{\mathrm{r}}, p_2^{\mathrm{r}}, \ldots, p_N^{\mathrm{r}}]^T$ and $\mathbf{p}^{\mathrm{l}} = [p_1^{\mathrm{l}}, p_2^{\mathrm{l}}, \ldots, p_M^{\mathrm{l}}]^T$ were assigned. In order to define the desirable selective features, the

$T : \mathbf{p}^{r} \rightarrow \mathbf{t}$ transformation was done. In this transformation, **t** is the image of the $\mathbf{p}^{r}$ vector in the form of a vector with coordinates corresponding to the $\mathbf{p}^{l}$ vector. For the transparent record of the transformation above with the use of vectors $\mathbf{p}^{r}$ and $\mathbf{p}^{l}$, the mapping was written in the Euclidean plane, that is, $T : E^{1} \rightarrow E^{2}$. In the issue, which is considered here, these transformations are linear mappings, so they can be written in the matrix form as $\mathbf{t} = T(\mathbf{p}^{p}, \mathbf{A})$, in which **A** is the matrix of a given transformation. Depending on the received symmetry or asymmetry (right/left-hand) of measurement points, they will create different dispersion graphs. An example of right-side and left-side asymmetry dispersion graph is presented in **Figures 9** and **10** and precisely described in the work of Dudczyk [13]. The number of measurement points is chosen empirically and is a double value of the maximum filter's width of the IF frequency from the superheterodyne receiver, which is used in the measurement procedure, that is, 40 MHz. As a result of this assumption, the critical original number of measurement points is as follows N = M = 80.

Depending on the received symmetry or asymmetry (right/left-side) of measurement points, it is possible to create dispersion graphs. Measurement points presented in **Figure 11**, transformed and depicted together, form the so-called measurement function $K(f_n)$. **Figure 11** shows the

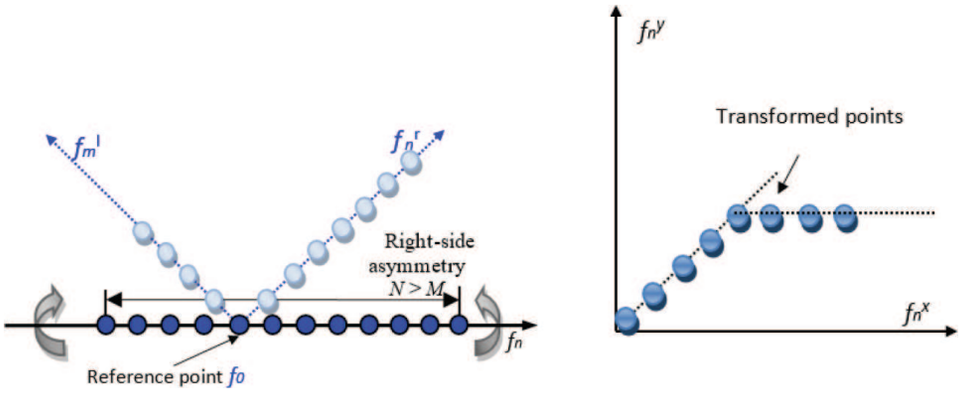

Figure 9. Depiction of transformation of measurement points in a 2D Euclidean space for N > M, that is, the range of right-hand asymmetry.

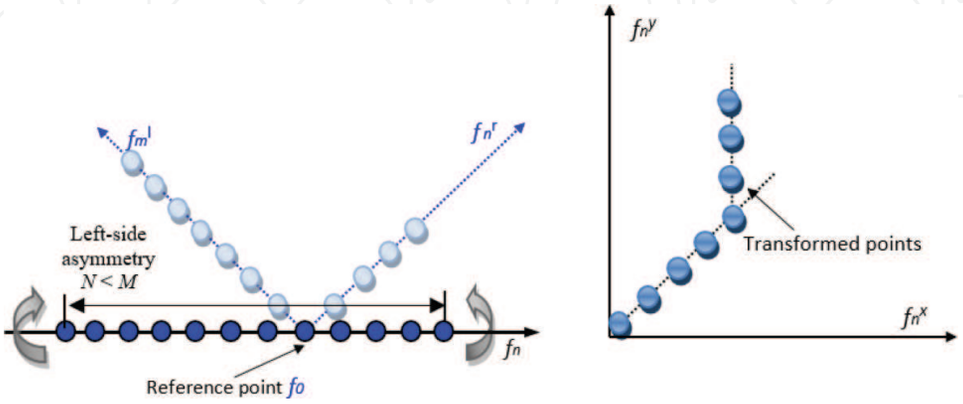

Figure 10. Depiction of transformation of measurement points in a 2D Euclidean space for N < M, that is, the range of left-hand asymmetry.

http://dx.doi.org/10.5772/67894

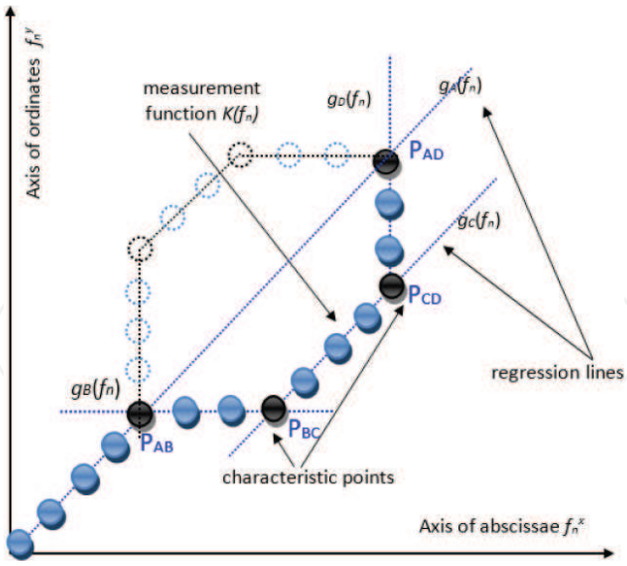

Figure 11. A graph of measurement points dispersion after transformation—attractor of transformation.

coordinate plane, where an abscissa (the value of x) is marked as a f_n^x and an ordinate (the value of y) is marked as a f_n^y.

On the basis of distinctive streaks that were formed, such hypothesis can be proposed: functions $g_A(f_n)$, $g_B(f_n)$, $g_C(f_n)$ and $g_D(f_n)$belong to the class of linear functions, in which$g_A(f_n)$, $g_B(f_n)$, $g_C(f_n)$and $g_D(f_n)$ will be the regression lines for the streaks formed through the measurement points [14]. Linear equation of regression for the presented case is defined with the following equation $\mathbf{g}(f_n) = \boldsymbol{\alpha} \cdot f_n + \boldsymbol{\beta}$, in which $\boldsymbol{\alpha}$ can be expressed as a vector $[\alpha_A, \alpha_B, \alpha_C, \alpha_D]^T$ and $\boldsymbol{\beta}$ can be expressed as a vector $[\beta_A, \beta_B, \beta_C, \beta_D]^T$ and $\mathbf{g}(f_n)$ can be expressed as a vector $[g_A(f_n), g_B(f_n), g_C(f_n), g_D(f_n)]^T$. To define the value of $\boldsymbol{\alpha}$ and $\boldsymbol{\beta}$, Eq. (5) should be minimalized.

$$E[f_n^Y - \boldsymbol{\alpha} \cdot f_n - \boldsymbol{\beta}]^2 = \min \tag{5}$$

$$\begin{cases} \dfrac{\partial}{\partial \alpha} E[f_n^Y - \boldsymbol{\alpha} \cdot f_n - \boldsymbol{\beta}]^2 = -2E[(f_n^Y - \boldsymbol{\alpha} \cdot f_n - \boldsymbol{\beta}) f_n] \\ \dfrac{\partial}{\partial \beta} E[f_n^Y - \boldsymbol{\alpha} \cdot f_n - \boldsymbol{\beta}]^2 = -2E[(f_n^Y - \boldsymbol{\alpha} \cdot f_n - \boldsymbol{\beta})] \end{cases} \tag{6}$$

After comparing the calculated derivatives Eq. (6) to zero, appears the system of normal equations in which after replacing the expected values with particular moments of equation systems, the following equation can be written:

$$\begin{cases} \boldsymbol{\alpha} \cdot m_{20} + \boldsymbol{\beta} \cdot m_{10} = m_{11} \\ \boldsymbol{\alpha} \cdot m_{10} + \boldsymbol{\beta} = m_{01} \end{cases} \tag{7}$$

in which m_{10} and m_{01} are sample *1*st moments, m_{20} is sample *2nd* moment and m_{11} is mixed sample *1st* moment. After further transformations, the regression equation is as follows:

$$g(f_n) = \frac{\mu_{11}}{\mu_{20}} \cdot f_n + \left(m_{01} - \frac{\mu_{11}}{\mu_{20}} m_{10} \right) = \boldsymbol{\alpha}_{21} f_n + \boldsymbol{\beta} \tag{8}$$

where

$$\boldsymbol{\alpha}_{21} = \left[\frac{\mu_{11}^A}{\mu_{20}^A}, \frac{\mu_{11}^B}{\mu_{20}^B}, \frac{\mu_{11}^C}{\mu_{20}^C}, \frac{\mu_{11}^D}{\mu_{20}^D} \right]^T = [\alpha_A, \alpha_B, \alpha_C, \alpha_D]^T \tag{9}$$

$$\boldsymbol{\beta} = \left[m_{01}^A - \frac{\mu_{11}^A}{\mu_{20}^A} m_{10}^A, m_{01}^B - \frac{\mu_{11}^B}{\mu_{20}^B} m_{10}^B, m_{01}^C - \frac{\mu_{11}^C}{\mu_{20}^C} m_{10}^C, m_{01}^D - \frac{\mu_{11}^D}{\mu_{20}^D} m_{10}^D \right]^T = [\beta_A, \beta_B, \beta_C, \beta_D]^T \tag{10}$$

and μ_{11} means mixed *2nd* central moment and μ_{20} means *2nd* central moment. As a result of further transformations, four linear regression equations were given. The particular equation system given by the regression equation allows to calculate characteristic points of coordinates. Examples of four characteristic points presented in **Figure 11** in the form of black points, such as (P_{AB}, P_{BC}, P_{CD}, P_{AD}), were formed. Then, with the use of characteristic points of coordinates, the measurement function $K(f_n)$ was formed.

4.2. Distinctive fractal features extraction

As a result of further transformations, four equations of linear regression were received. Then, it is possible to draw a measurement function $K(f_n)$ in the form of a product k degree given $k + 1$ characteristic points, defined by the Lagrange's polynomial formula in accordance with Eq. (11), where a_k, a_{k-1}, …, a_0 are characteristic parameters of measurement function $K(f_n)$, as shown in **Figure 12**.

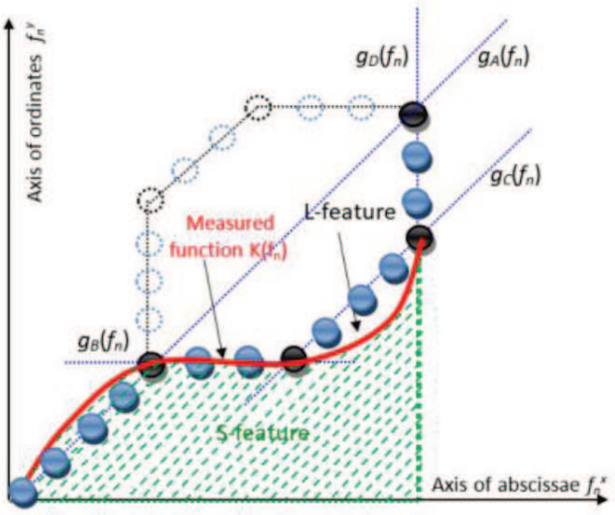

Figure 12. The image of measured function according to Lagrange polynomial and fractal features extraction.

$$K(f_n) = a_k f_n^k + a_{k-1} f_n^{k-1} + a_{k-2} f_n^{k-2} + \cdots + a_0 \tag{11}$$

The formalized notation of the measurement function $K(f_n)$ allows to extract distinctive features through defining the space area under the measurement function and the arc length of the function, which appeared for the SEI process. The feature S is the value of the space area of a closed surface expanding from the generalized measurement function $K(f_n)$ in the bracket $\langle f_n^{\min}, f_n^{\max} \rangle$, respecting Eq. (12).

$$S = \int_{f_n^{\min}}^{f_n^{\max}} K(f_n) df_n = \int_{f_n^{\min}}^{f_n^{\max}} (a_k f_n^k + a_{k-1} f_n^{k-1} + a_{k-2} f_n^{k-2} + \cdots + a_0) df_n \tag{12}$$

Simultaneously, the arc length of the generalized measurement function $K(f_n)$ as the second distinction feature of the radar emission source will be represented through the arc length L of the function $K(f_n)$ in the brackets $\langle f_n^{\min}, f_n^{\max} \rangle$, respecting Eq. (13).

$$L = \int_{f_n^{\min}}^{f_n^{\max}} \left[1 + \left(\frac{\partial K(f_n)}{\partial f_n} \right)^2 \right]^{\frac{1}{2}} df_n = \int_{f_n^{\min}}^{f_n^{\max}} \left[1 + \left(k a_k f_n^{k-1} + (k-1) a_{k-1} f^{k-2} + \ldots + a_1 \right)^2 \right]^{\frac{1}{2}} df_n \tag{13}$$

According to Eqs. (12) and (13), it is possible to extract two additional distinctive features, that is, the length of measurement function and the value of area which is included under this function. The presented method of features extraction makes it possible to estimate numerical surface areas under the measurement functions (feature S) and the distance of arc of these functions (feature L). Then the vector of basic measurable parameters of radar signal was extended with two additional features.

Given in that way, two additional features expand the $\mathbf{V_B}$ vector of the basic features of radar signal measurable parameters, such as PW, PRI and RF. And these features are a good separation measure in the SEI process. The way of defining these two additional features and using them in the process of identification of the radar copies of the same type was presented in further part of this chapter.

5. Fractal of generalized measurement function

Generalization of the method of radar signal identification on the basis of the transformation fractal is defining the generalized measurement function $\hat{K}(f_n)$ going through all particular characteristic points P_n, in which $n = 0,1,\ldots,k_{gr}$. **Figure 13** presents the fractal character of the measurement function received as a result of the transformation of the set of measurement points.

The generalized measurement function $\hat{K}(f_n)$ preserves the character of not decreasing function in a particular bracket $\langle f_n^{\min}, f_n^{\max} \rangle$ and out of definite character, it shows prediction

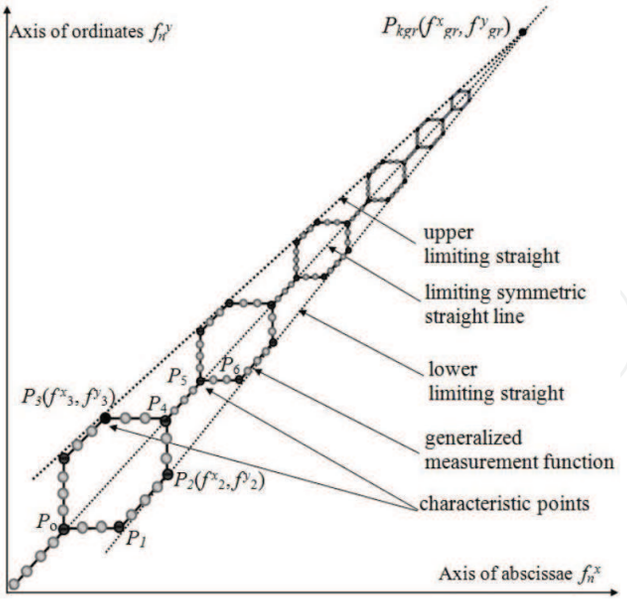

Figure 13. The fractal character of generalized measurement function.

features. Simultaneously, $\hat{K}(f_n)$ is located in an area that is mapped by the lower limiting straight $F_L(f_n)$ and upper limiting straight $F_U(f_n)$ and is symmetric relatively to the symmetrical limiting straight $F_S(f_n)$ according to Eqs. (14)–(16), in which f_2^x, f_3^x, f_{gr}^x are the abscissae of characteristic points and f_2^y, f_3^y, f_{gr}^y are the ordinates of characteristic points. **Figure 13** presents a fractal character of the generalized measurement function which has the form of a contraction mapping.

$$F_L(f_n) = \left[\frac{f_{gr}^y - f_2^y}{f_{gr}^x - f_2^x}\right] \cdot (f_n - f_2^x) + f_2^y \tag{14}$$

$$F_U(f_n) = \left[\frac{f_{gr}^y - f_3^y}{f_{gr}^x - f_3^x}\right] \cdot (f_n - f_3^x) + f_3^y \tag{15}$$

$$F_S(f_n) = \left[\frac{f_{gr}^y}{f_{gr}^x}\right] \cdot f_n \tag{16}$$

It should be mentioned that the received shape of the measurement function (according to **Figures 11** and **12**) is an individual model of a radar emission source. 'An individual model' means 'lines on the fingers' of the radar which make a clear identification possible.

6. Results of analysis

To compare the received results with other RSR methods based on, for example, Fast decision Identification Algorithm of emission source pattern described in Ref. [6], or out-of-band

radiation of radar devices described in Ref. [13], or inter-pulse modulation described in Ref. [7] and intra-pulse analysis of a radar signal shown in Ref. [15] or method based on data modelling presented in Ref. [16], Correct Identification Coefficient (CIC) is set according to Eq. (17), where n_{B-P} is the number of correct comparisons of basic features' vectors $\mathbf{V_B}$ (presented according to Eq. (4)), to extended vectors $\mathbf{V_{EXT}}$ (with two additional features L and S) in a particular class, where N is the number of all comparisons divided by the number of test collections.

$$\mathrm{CIC} = \frac{n_{B-P}}{N} \tag{17}$$

The number of n_{B-P} correct comparisons is set according to Eq. (18), where γ_i^j function assigns to a pair of vectors $(\mathbf{V}_\mathrm{B}^i, \mathbf{V}_{EXT}^j)$ the value which equals '1' if i = j, or the value which equals '0' if $i \neq j$. The example of CIC received values are presented in the following part of this chapter.

$$n_{B-P} = \sum_{i=1}^{I}\sum_{j=1}^{J}\gamma^{i\,j} \tag{18}$$

The process of identification was made on the basis of length measurement and the decision about the criterion of minimal distance classification. A correctness estimation of tests with particular class were Mahalanobis, Euclidean and Hamming distances (metrics) [17, 18]. The criterion of classification was the criterion of 'the nearest neighbour', which was used as one of the basic threshold criteria [19]. In order to assess the quality of the classification/identification process, the Correct Identification Coefficient was defined.

According to Eqs. (8) and (9), it was possible to extract two additional distinctive features, that is, the length of measurement function and the value of area which is included under this function. The results were presented in **Figures 14–16**.

Also, the received estimation results are presented in **Figures 17–19**. Appropriately crossed columns and lines of each $\mathbf{V}_\mathrm{B}$ vector and extended vectors $\mathbf{V_{EXT}}$ present the degree of their similarity defined by the distance value. The less value of this distance means the bigger similarity of $\mathbf{V}_\mathrm{B}$ vector to the extended vectors. Also, in **Figures 15–17**, there are minimum values of the distance marked with a red dotted ellipse.

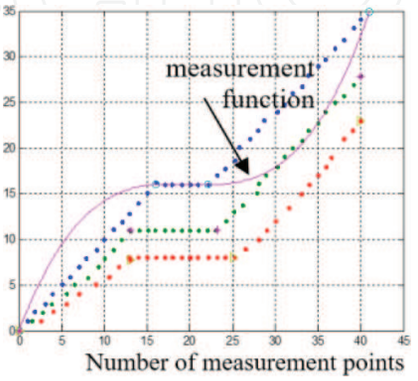

Figure 14. An attractor of transformation for Copy of Radar No. 1.

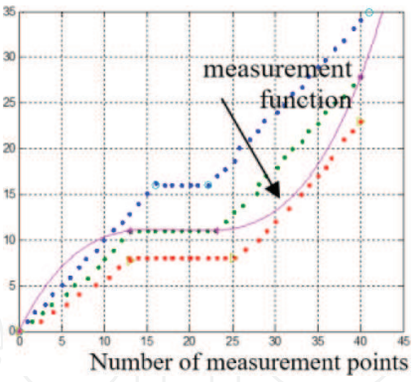

Figure 15. An attractor of transformation for Copy of Radar No. 2.

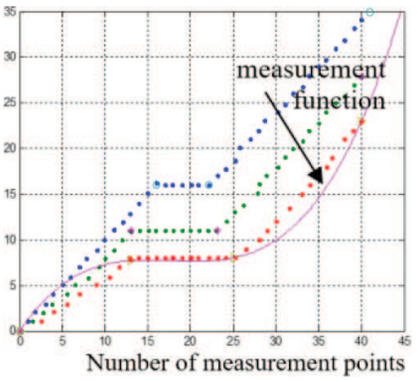

Figure 16. An attractor of transformation for Copy of Radar No. 3.

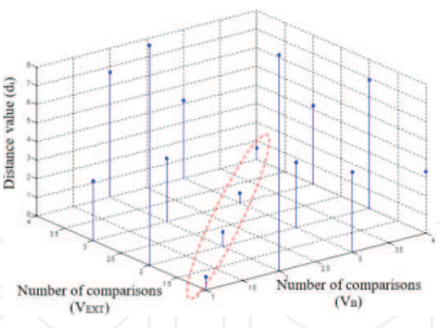

Figure 17. The values of Mahal distances for Radar Copy No. 1.

A correctness estimation of tests with particular class were Mahalanobis, Euclidean and Hamming distances (metrics) [21]. The SEI estimation results are presented in **Figures 20–22**.

According to the SEI methods listed in this chapter, the received RER results are as follows: the use of out-of-band radiation described in the work of Dudczyk [13] and the CIC value for RSR is about 90%. The method based on fractal features described in the work of Dudczyk and Kawalec [3], and the CIC value is 91.6% for Mahalanobis metric and 96.7% for Euclidean and Hamming metrics. Very similar RER results are received in the work of Dudczyk and Kawalec

http://dx.doi.org/10.5772/67894

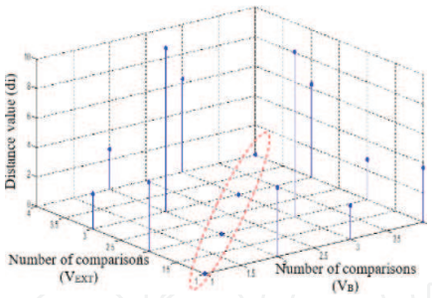

Figure 18. The values of Mahal distances for Radar Copy No. 2.

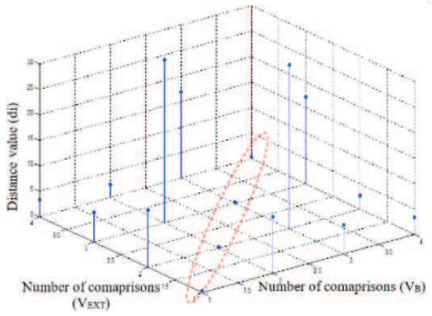

Figure 19. The values of Mahal distances for Radar Copy No. 3.

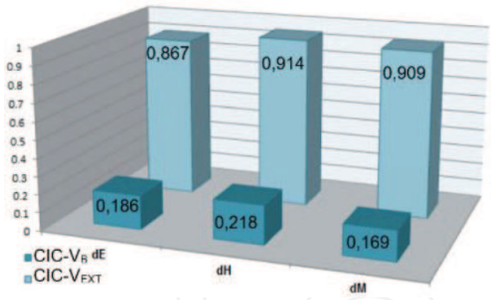

Figure 20. The values of CIC for Radar Copy No. 1.

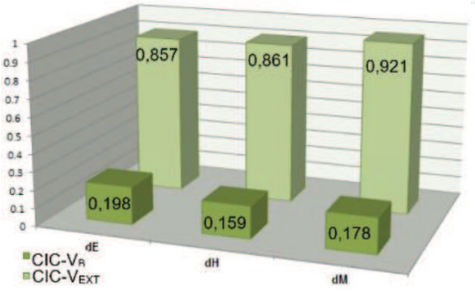

Figure 21. The values of CIC for Radar Copy No. 2.

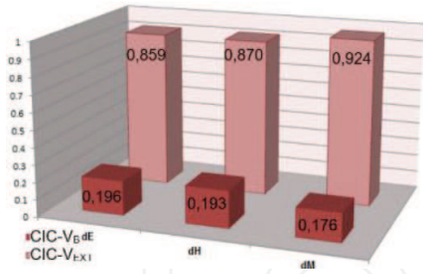

Figure 22. The values of CIC for Radar Copy No. 3.

[4], where RSR is also based on the analysis of fractal features. The method based on inter-pulse analysis described in the work of Dudczyk et al. [7] increases the CIC coefficient up to 70%, and the method based on intra-pulse analysis described in the work of Kawalec and Owczarek [15] makes it possible to receive RSR results reaching 90% level. Data modelling applied to RSR and identification is presented in the work of Kawalec and Owczarek [16]. In this work, the value of CIC equals 98%. In the work of Dudczyk and Kawalec [6], the Fast Identification Algorithm for RER is presented. This algorithm is parameterized in three stages by implementation of three different ways to define the similarity degree of the signal vector to the pattern in the database. Based on this algorithm, the CIC value is 63%. In order to depict it, in **Figure 23**, there have been presented CIC values.

The presented method of features extraction makes it possible to estimate numerical surface areas under the measurement functions (feature *S*) and the distance of arc of these functions (feature *L*). Then, the vector of basic measurable parameters of radar signal was extended with two additional features. Given in that way, two additional features expand the vector of the basic features of radar signal measurable parameters, such as PW, PRI and RF, are a good separation measure in the SEI process. The way of defining these two additional features and using them in the process of identification of the radar copies of the same type was presented. The features S and L are distinctive information for good separating measure in the SEI process. Simultaneously, as a result of transformations in collections of measurement points,

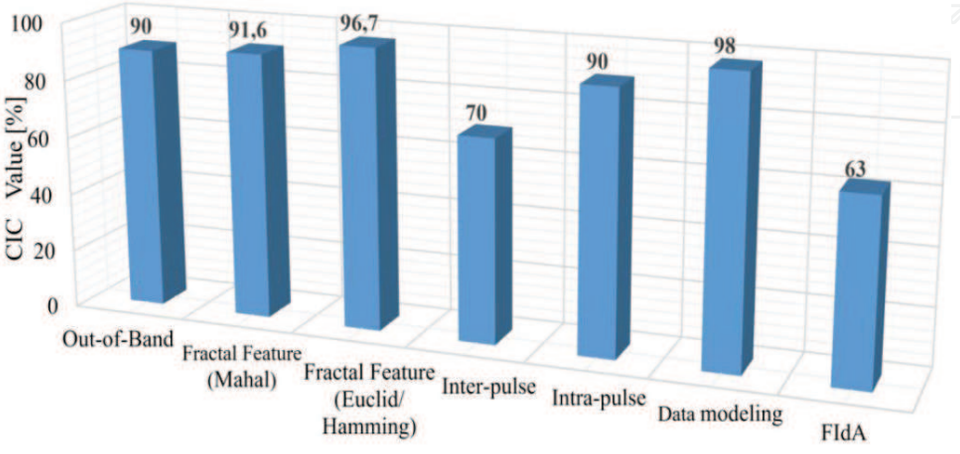

Figure 23. Graphic illustration of CIC values for other RER methods.

the transformation attractor of the generalized measurement function is received. The received attractor is used later on to optimize the SEI process.

It needs to be emphasized with full conviction that referring to the works above, during the SEI procedure, the same recordings of a few hundred radar signals coming from the same type of radars are used. Only by this approach, it is possible to compare the received results. It needs to be emphasized that the RSR methods listed in this chapter differ from each other as concerns the test procedure, the compilation level, calculation time and algorithm complexity. However, the main difference is that in the process of generating distinctive features, it is possible to achieve different distinctive features from a radar signal. In that way, a quasi-optimum radar signal pattern appeared.

7. Conclusion

Radar signal recognition with the use of classical methods, that is, based on statistical analysis of basic measurable parameters of a radar signal, such as radio frequency, amplitude, pulse width or pulse repetition interval, is not enough to carry out the distinction process of particular copies of the same radar type.

The received measurement data have a significant influence on the SEI process of radar, in which it is aimed to receive very high level of radar signal identification. Ultimately, signal source identification, which is 100%, should be characterized by the maximization of explicitness of RER procedure. It is not a trivial matter to achieve such a result. It is also known that stochastic context-free grammars (SCFG) appear promising for the recognition and threat assessment of complex radar emitters in radar systems, but the computational requirements for learning their production rule probabilities can be very onerous [20]. As shown in Ref. [21], a self-organizing map and the maximum likelihood gamma mixture model classifier and adopted Bayesian formalism are too complicated for direct analytical use in automatic radar recognition. The presented SEI method based on fractal features is realized on the basis of MatLab software package and received vectors are recorded in a dedicated database for ELINT system. The received CIC value indicates that there has been a noticeable rise in the radar signal correct identification. Comparing the received results of the identification process with other methods, it may be admitted that the presented method makes it possible to increase the value of CIC. In order to increase the CIC coefficient value, in further works on RSR use in SEI process, a common similarity matrix should be defined. This matrix should include the complexity of algorithms which are used in the RER method, estimation time, the requirements of the equipment platform and other requirements, which are significant in the process of quality estimation of a particular method. Thus, it will be possible to count automatically the similarities between vectors of basic measurable parameters for different radar copies of the same type. For ELINT systems working in real conditions, on a contemporary battlefield, the automation of RSR process and explicit identification of every single emitter in real time (with minimum time burden) are currently primary challenges for ELINT specialists

This chapter highlights the fact that the RSR process described here is a complex problem. It is also generally known that a number of aspects such as defining the DataBase, the method

which creates the pattern, classification process and identification process, the criteria which are used and the method to calculate the correct identification coefficient, are currently a great challenge for researchers and, for the time being, there are no optimal solutions to them. Many solutions are still a mystery in this subject and because of the fact that they are a matter of current EW field and specific programme-device applications, they cannot be published. All attempts to implement such solutions to ELINT systems and electronic warfare should be optimized to a particular device not to overload the SEI system.

Author details

Janusz Dudczyk

Address all correspondence to: j.dudczyk@wb.com.pl

WB Electronics S.A., R&D Department, Poznanska, Poland

References

[1] J. Dudczyk. Radar emission sources identification based on hierarchical agglomerative clustering for large data sets. Journal of Sensors. 2016;**2016**(2016):1879327. doi:10.1155/2016/1879327

[2] J. Dudczyk, A. Kawalec. Specific emitter identification based on graphical representation of the distribution of radar signal parameters. Bulletin of the Polish Academy of Sciences, Technical Sciences. 2015;**63**(2):391–396. doi:10.1515/bpasts-2015-0044

[3] J. Dudczyk, A. Kawalec. Fractal features of specific emitter identification. Acta Physica Polonica. 2013;**124**(3):406–409. doi:10.12693/APhysPolA.124.406

[4] J. Dudczyk, A. Kawalec. Identification of emitter sources in the aspect of their fractal features. Bulletin of the Polish Academy of Sciences, Technical Sciences. 2013;**61**(3):623–628. doi:10.2478/bpasts-2013-0065

[5] J. Dudczyk, A. Kawalec. The use of fractal features extracted from radar signals in the process of specific identification. Przegląd Elektrotechniczny. 2014;**R.90**(11/2014):212–215. doi:10.12915/pe.2014.11.54

[6] J. Dudczyk, A. Kawalec. Fast-decision identification algorithm of emission source pattern in database. Bulletin of the Polish Academy of Sciences, Technical Sciences. 2015;**63**(2):385–389. doi:10.1515/bpasts-2015-0043

[7] J. Dudczyk, J. Matuszewski, A. Kawalec. Specific emitter identification based on an interpulses modulation of radar signals. Przegląd Elektrotechniczny. 2016;**R.92**(9/2016):267–271. doi:10.15199/48.2016.09.64

[8] F. Berizzi, G. Bertini, M. Martorella. Two-dimensional variation algorithm for fractal analysis of sea SAR images. IEEE Transactions on Geoscience and Remote Sensing. 2006;**44**(9):2361–2373. doi:10.1109/TGRS.2006.873577

[9] M. German, G.B. Bénié, J.M. Boucher. Contribution of the fractal dimension to multiscale adaptive filtering of SAR imagery. IEEE Transactions on Geoscience and Remote Sensing. 2003;**41**(8):1765–1772. doi:10.1109/TGRS.2003.811695

[10] B. Świdzińska. Fractal compression using random encoding algorithm. Bulletin of the Polish Academy of Sciences, Technical Sciences.1998;**46**(4):525–532. ISSN 0239-7528

[11] A. Wojtkiewicz, M. Nałęcz, K. Kulpa, R. Rytel-Andrianik. A novel approach to signal processing in FMCW radar. Bulletin of the Polish Academy of Sciences, Technical Sciences. 2002;**50**(4):347–359. ISSN 0239-7528

[12] K.I. Talbot, P.R. Duley, M.H. Hyatt. Specific emitter identification and verification. Technology Review Journal Spring/Summer 2003:113–133.

[13] J. Dudczyk. Applying the radiated emission to the radio-electronic devices identification. Dissertation thesis, Department of Electrical, Military University of Technology, Poland; 2004, (in Polish).

[14] Z. Hellwig. Theory of probability and mathematical statistics. Warsaw: Scientific Press PWN; 1998.

[15] A. Kawalec, R. Owczarek. Radar emitter recognition using intrapulse data. In Proceedings of the NordSec 2005—The 10th Nordic Workshop on Secure IT-Systems, pp. 444–457, Warsaw, Poland, 17–19 May 2004.

[16] A. Kawalec, R. Owczarek, J. Dudczyk. Data modelling and simulation applied to radar signal recognition. Molecular and Quantum Acoustics. 2005;**26**:165–173.

[17] R.O. Duda, P.E. Hart, D.G. Stork. Pattern classification (2nd ed.). New York: John Wiley & Sons; 2000.

[18] K. Fukunaga. Introduction to statistical pattern recognition (2nd ed.). New York: Academic Press; 1990.

[19] C.T. Zahn. Graph-theoretical methods for detecting and describing gestalt clusters. IEEE Transactions on Computers. 1971;**1**:68–86.

[20] G. Latombe, E. Granger, F. Dilkes. Fast learning of grammar production probabilities in radar electronic support. IEEE Transactions on Aerospace and Electronic Systems. 2010;**46**: 1262–1289.

[21] K. Copsey, A. Webb. Bayesian gamma mixture model approach to radar target recognition. IEEE Transactions on Aerospace and Electronic Systems. 2003;**39**:1201–1217.

IntechOpen